Surface hopping with cumulative probabilities: even sampling and improved reproducibility

Shane M. Parker[a] and Colin J. Schiltz

Department of Chemistry, Case Western Reserve University

10800 Euclid Ave, Cleveland, OH 44106, USA

(Dated: 9 October 2020)

Trajectory surface hopping simulations of photochemical reactions are a powerful and increasingly important tool to unravel complex photochemical reactivity. Within surface hopping, electronic transitions are mimicked by stochastic hops between electronic potential surfaces. Thus, statistical sampling is an inescapable component of trajectory-surface-hopping-based nonadiabatic molecular dynamics methods. However, the standard sampling strategy inhibits computational reproducibility, limits predictability, and results in trajectories that are overly sensitive to numerical parameters like the time step. We describe an equivalent approach to sampling electronic transitions within fewest switches surface hopping (FSSH) in which hops are decided in terms of the cumulative probability (FSSH-c) as opposed to usual prescription, which is in terms of the instantaneous conditional probability (FSSH-i). FSSH-c is statistically equivalent to FSSH-i and can be implemented from trivial modifications to an existing surface hopping algorithm, but has several key advantages: i) a single trajectory is fully specified by just a handful of random numbers, ii) all hopping decisions are independent of the time step such that convergence behavior of individual trajectories can be explored, and iii) alternative integral-based sampling schemes are enabled. In addition, we show that the conventional hopping probability overestimates the hopping rate and propose a simple scaling correction as a fix. Finally, we demonstrate these advantages numerically on model scattering problems.

[a]Electronic mail: shane.parker@case.edu

I. INTRODUCTION

Mixed quantum-classical nonadiabatic molecular dynamics[1–3] (NAMD) has emerged as an efficient and powerful tool to study processes involving electronic nonadiabaticity such as photochemical reactions[4], reactive scattering on metal surfaces[5,6], or chemical reactions in cavities.[7–9] Of the many approaches to NAMD reported previously, algorithms based on the trajectory surface hopping concept are especially advantageous because the independent trajectory approximation makes them amenable to on-the-fly molecular dynamics simulations, in which the energies, forces, and nonadiabatic couplings required to propagate trajectories are computed at each time step using semiempirical or ab initio electronic structure methods. In particular, NAMD simulations powered by time-dependent density functional theory[10–23] appear to strike an ideal balance between computational cost and accuracy of the potential energy surfaces.

The Fewest Switches Surface Hopping (FSSH) approach to trajectory surface hopping is perhaps the most widely used.[24] Within FSSH, the nuclear degrees of freedom are treated classically and the forces governing nuclear motion come from a single (usually adiabatic) potential energy surface. Electronic transitions are included in the form of "hops" between potential energy surfaces. Intense interest in nonadiabatic dynamics in general and photochemistry in condensed systems in particular has led to substantial progress[25] towards curing FSSH's principal pathologies, such as an inconsistent nuclear-electronic coherence[26–29], and an unphysical dependence on the electronic representation[30,31]. In addition, surface hopping algorithms that incorporate coupled trajectories have been recently introduced,[32,33] as well as algorithms that target electronic coherences on the same footing as electronic populations.[34] Since the cost of an FSSH simulation is directly proportional to the number of trajectories sampled, reducing the number of trajectories required for a desired accuracy can have a significant impact on feasibility. The army ants algorithm, for instance, enables FSSH for rare events (e.g., probability of 10^{-6}) by artificially increasing low hopping probabilities and compensating by reweighting trajectories.[35] Similarly, importance sampling has been applied to the sampling of the initial conditions and shown to greatly reduce the number of independent initial conditions needed to be sampled to study the influence of temperature on photoabsorption cross sections.[36]

As originally proposed, hops in FSSH are decided by computing an instantaneous hopping probability at each time step and comparing the hopping probability to a random number.[24] Within FSSH, the hopping probabilities are chosen such that on average, the proportion of trajectories on

a given potential energy surface matches the electronic population of that state. Consequently, the FSSH algorithm inherently requires sampling with independent trajectories. Of course, deterministic approaches to simulating surface hopping trajectories could be used instead. For example, the ants algorithm for trajectory surface hopping—which predates FSSH—deterministically spawns new trajectories at specified decision points and weights the new trajectories according to the instantaneous hopping probability.[35,37] A similar approach is used in full multiple spawning (FMS), a deterministic trajectory-based nonadiabatic molecular dynamics method spawns new trajectories in regions of strong vibronic coupling.[38] However, such spawning algorithms can become impractical for long simulations because the number of trajectories (and therefore the computational cost) grows exponentially as a function of simulation time.[35] Stochastic approaches remain advantageous because they let one control the computational cost without biasing the results. For example, the recently proposed stochastic-selection approach to ab initio multiple spawning[39] stochastically discards trajectory basis functions during a simulation and thereby avoids the exponential growth in the number of trajectories encountered in the deterministic ab initio multiple spawning.[38]

The stochastic nature of FSSH poses several obstacles to the reproducibility of simulations performed using different implementations because direct comparisons are only possible between implementations using the same classical integrator, electronic propagator, and sequence of random numbers. We specifically refer here to computational reproducibility, which has been defined as "obtaining consistent results using the same input data, computational methods, and conditions of analysis."[40] FSSH results must be reproduced in a statistical sense, meaning many trajectories must be simulated and estimated properties of the distributions must be compared, which can require thousands to millions of trajectories depending on the desired precision. By contrast, with deterministic trajectory methods, independent implementations of the same method can often generate identical results down to machine precision on just a single trajectory. An illustrative example is the question of whether a coin flip is fair; almost 10000 independent coin flips would be required to have a 95% confidence that the bias in a given coin is less than 0.01. Thus, computational reproducibility can be enhanced by reducing or limiting the influence of stochasticity in a computational method.

Similarly, numerically confirming convergence behavior of FSSH algorithms with respect to time step is challenging because random numbers are drawn for each time step such that changing the classical time step necessarily changes the hopping behavior. For this reason, convergence with respect to time step is investigated rarely and always in a statistical sense.[41,42]

Here, we introduce an alternative criterion for deciding surface hops in FSSH based on the cumulative hopping probability, i.e., the probability of any hop occurring since the start of the simulation or the last hop. The cumulative viewpoint is inspired by the perturbative expansion of semiclassical time-dependent molecular wavefunction in powers of the nonadiabatic coupling by White et al[43,44], in which the molecular wavefunction is expanded as an infinite series ordered according to the number and times of all possible surface hops. Similar expressions were used by others to expand the quantum-classical Liouville equation.[45,46] However, the cumulative algorithm we propose is nonperturbative.

In addition to significantly reducing the number random numbers needed to propagate a single trajectory, using the cumulative hopping probability carries two more significant advantages. First, it removes any dependence of surface hopping decisions on the time step so that convergence of single trajectories with respect to the time step can be studied numerically. Second, the cumulative point-of-view allows one to rewrite the results of a swarm of surface hopping trajectories as an integral on the unit hypercube, which is especially amenable to numerical integration techniques.

This paper is organized as follows. In Sec. II we review the basic structure of FSSH so that we can introduce the FSSH-i and FSSH-c algorithms. In addition, we sketch an even sampling algorithm obtained from integrating the surface hopping hypercube with a quadrature. In Sec. III we use a python implementation to show that FSSH-c yields identical dynamics as FSSH-i. With this implementation, we numerically demonstrate that the convergence behavior of a single trajectory can be studied. We then show that the even sampling algorithm significantly reduces statistical noise in swarms of trajectories. Finally, we conclude in Sec. IV by discussing several avenues of ongoing research.

II. FEWEST SWITCHES SURFACE HOPPING (FSSH)

In mixed quantum-classical nonadiabatic molecular dynamics (NAMD) methods, the electronic subsystem is treated quantum mechanically by expanding in a few-state electronic basis and the nuclear subsystem is treated classically.[24] We write the vector of nuclear positions as $\mathbf{R}(t)$. The electronic wavefunction is typically expanded in a nuclear-position-dependent basis as

$$|\Psi(t)\rangle \equiv \sum_n c_n(t)|\Phi_n;\mathbf{R}(t)\rangle \tag{1}$$

where $c_n(t)$ are time-dependent expansion coefficients, and $|\Phi_n; \mathbf{R}(t)\rangle$ is the n-th many-electron state which depends parametrically on the nuclear position. Alternatively, the electronic density operator

$$\hat{\sigma}(t) \equiv \sum_{nm} \sigma_{nm}(t) |\Phi_n; \mathbf{R}(t)\rangle\langle\Phi_m; \mathbf{R}(t)| \tag{2}$$

can also be used directly. The many-electron states are often chosen to be adiabatic states, i.e., states that satisfy

$$\hat{H}_{\mathbf{R}} |\Phi_n; \mathbf{R}\rangle = E_n(\mathbf{R}) |\Phi_n; \mathbf{R}\rangle, \tag{3}$$

where $\hat{H}_{\mathbf{R}}$ is the electronic Hamiltonian with nuclei fixed at positions $\mathbf{R}$ and $E_n(\mathbf{R})$ are potential energy surfaces, but other choices, including diabatic states are also permissible.

The expansion coefficients are propagated according to the time-dependent Schrödinger equation with

$$\dot{\mathbf{c}}(t) = -i \left(\mathbf{H}(t) - i\mathbf{W}(t)\right) \mathbf{c}(t) = -i\bar{\mathbf{H}}(t)\mathbf{c}(t) \tag{4}$$

or

$$\dot{\boldsymbol{\sigma}}(t) = -i[\bar{\mathbf{H}}, \boldsymbol{\sigma}(t)], \tag{5}$$

where $\bar{\mathbf{H}} = \mathbf{H}(t) - i\mathbf{W}(t)$ and the elements of the matrix $\mathbf{H}$ (the electronic Hamiltonian) and $\mathbf{W}$ (the nonadiabatic coupling) are

$$H_{nm}(t) = \langle\Phi_n; \mathbf{R}(t)|\hat{H}_{\mathbf{R}(t)}|\Phi_m; \mathbf{R}(t)\rangle \tag{6}$$

$$W_{nm}(t) = \langle\Phi_n; \mathbf{R}(t)|\frac{\partial}{\partial t}|\Phi_m; \mathbf{R}(t)\rangle = \boldsymbol{\tau}_{nm} \cdot \dot{\mathbf{R}}. \tag{7}$$

In the previous equation,

$$\boldsymbol{\tau}_{nm} \equiv \langle\Phi_n; \mathbf{R}(t)|\nabla_{\mathbf{R}}\Phi_m; \mathbf{R}(t)\rangle \tag{8}$$

is the first-order derivative coupling vector and $\dot{\mathbf{R}}$ is the nuclear velocity.

The defining characteristics of all surface hopping methods are that i) at all times during a trajectory the classical nuclei feel forces corresponding to a single potential energy surface referred to as the active surface or active state and ii) electronic transitions are mimicked through stochastic "hops" between different electronic states and hence different potential energy surfaces.[24] In particular, the FSSH variant is defined by choosing the rate of electronic transitions such that the number of hops is minimized and for an ensemble of independent trajectories—referred to as a swarm—the proportion of trajectories on any given state matches the electronic population of that

state on average. In other words, the rate of electronic transitions is chosen such that

$$\frac{\langle N_k \rangle}{N_{\text{traj}}} \to |c_k|^2, \tag{9}$$

where $\langle N_k \rangle$ is the average number of trajectories in a swarm of N_{traj} independent trajectories with active state k.

After a hop has been initiated, regardless of the criterion used to decide on a hop, the kinetic energy of the nuclei is adjusted to conserve total energy by scaling the nuclear momentum in the direction of the derivative coupling, $\boldsymbol{\tau}$. If there is insufficient nuclear kinetic energy parallel to the direction of the derivative coupling, then the hop is aborted. This is referred to as a frustrated hop. In our implementation, no additional action is taken for a frustrated hop (i.e., the trajectory continues with no momentum reversal).

A. FSSH with instantaneous probabilities (FSSH-i)

According to the original prescription, hops are decided in each time interval from t to $t + \Delta t$ by computing the probability of hopping from the active state k to another state n,

$$p_{k\to n}(t, t + \Delta t) = g_{k\to n}(t)\Delta t, \tag{10}$$

where

$$g_{k\to n}(t) = \sigma_{nk}(t)\bar{H}_{kn}(t) - \bar{H}_{nk}(t)\sigma_{kn}(t) \tag{11}$$

is the instantaneous hopping probability and Δt is the time step. In practice, a uniform random number $\eta \in \mathcal{U}(0, 1)$ is drawn and a hop is initiated if $\eta < p_{k\to n}$. Thus, the total number of random numbers drawn over the course of a trajectory is N_{steps}, a purely numerical parameter. We refer to this scheme as FSSH with instantaneous probabilities (FSSH-i) and it is depicted in Fig. 1.

We show in this paper that Eq. (10) overestimates the hopping rate when $p_{k\to n}(t, t+\Delta t)$ becomes large. To illustrate why Eq. (10) overestimates the actual hopping probability, consider a time interval $(t, t + \Delta t)$ for which $g_{k\to n}(t)\Delta t = \frac{1}{2}$ and assume $g_{k\to n}$ is constant in the time interval. This straightforwardly leads to an overall branching probability

$$\text{hop prob.} \in (t, t + \Delta t) \to \frac{1}{2},$$

i.e., half of all trajectories should hop in the time interval $(t, t + \Delta t)$. Now consider the branching probability if two half steps were performed such that the hopping probability in each step becomes

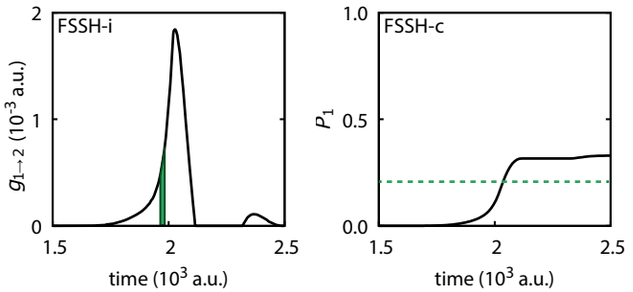

FIG. 1. Instantaneous (left) and cumulative (right) hopping probabilities for a scattering simulation on Tully's simple avoided crossing model. In FSSH-i (left), hopping decisions are made based on integrated instantaneous hopping probabilities such as the indicated region. In FSSH-c (right), hops are initiated when the cumulative probability crosses a randomly chosen threshold signified by the horizontal dashed line.

$\frac{1}{4}$, but each step has an independent hopping probability. The total probability of the trajectory hopping in $(t, t + \Delta t)$ is thus

$$\text{hop prob.} \in (t, t+\Delta t) \to \frac{1}{4} + \left(1 - \frac{1}{4}\right)\frac{1}{4} = 0.4375,$$

which is the probability of a hop in the first step plus the probability of no hop in the first step but a hop in the second step. Hence, reducing the time step drastically reduces the branching probability in the $(t, t + \Delta t)$ time interval, even though $g_{k\to n}(t)$ was assumed to be constant. We can generalize this procedure by dividing the time interval into ℓ equal length segments, writing the probability of hopping in terms of the probability of no hop occurring in each time interval, $(1 - g_{k\to n}\Delta t/\ell)^\ell$, and evaluating the limit as ℓ goes to infinity,

$$\text{hop prob.} \in (t, t+\Delta t) \to 1 - \lim_{\ell\to\infty}\left(1 - \frac{g_{k\to n}\Delta t}{\ell}\right)^\ell = 1 - e^{-g_{k\to n}\Delta t},$$

where we have used the identity $\lim_{\ell\to\infty}\left(1 + \frac{x}{\ell}\right)^\ell = e^x$. Note that Eq. (10) is the first-order result of the previous equation. Therefore, we propose a simple scaling correction to Eq. (10),

$$p_{k\to n}(t, t+\Delta t) = s(g_k\Delta t)g_{k\to n}(t)\Delta t, \tag{12}$$

where

$$s(x) = \frac{1 - e^{-x}}{x}, \tag{13}$$

$$g_k = \sum_{n\neq k} H(g_{k\to n}(t)) \tag{14}$$

is the instantaneous probability of any hop occurring to any state and H is the Heaviside function that ensures that a hop to state n only occurs when the population of state n is increasing. Interestingly, this scale guarantees the hopping probabilities are less than 1, which is a requirement for proper probabilities violated by Eq. (10). In addition, Eq. (12) correctly gives the same overall hopping probability whether using one step or two half steps. Using the same example as above where $g_k \Delta t = \frac{1}{2}$, the probability of hopping over two half steps is $(1 - e^{-1/4}) + e^{-1/4}(1 - e^{-1/4}) = 1 - e^{-1/2}$, which is identical to the single step hopping probability. For very small arguments, $s(x) \approx 1$, and the scaled result is nearly the same as Eq. (10). However, $s(x)$ decreases rapidly as x gets larger. For example, $s(0.02) \approx 0.99$, $s(0.1034) \approx 0.95$, and $s(0.215) \approx 0.9$, meaning when Eq. (10) indicates a 22% probability of hopping, $s(x)$ reduces that by a significant 10%. In situations where Eq. (10) guarantees a hop (i.e., the probability is equal to 1), $s(x)$ reduces it to a 63% probability. To avoid a problematic division by (near) zero, we evaluate $s(x)$ with a fourth-order Taylor series when $|x| < 10^{-3}$. Trajectories using this scaled probability are referred to as FSSH-i with Poisson probabilities because the probabilities follow a Poisson process and are denoted FSSH-ip.

B. FSSH with cumulative probabilities (FSSH-c)

Establishing the cumulative approach to FSSH starts with the recognition that $p_{k\to n}$ is formally the *conditional* probability that there is a hop in the time window $(t, t + \Delta t)$ given that there was no hop in the time window (t_0, t), where t_0 is a reference time such as the start of the simulation or the time of the most recent hop. The *cumulative* probability of a hop occurring since the reference time, $P_k(t_0, t)$, is a more convenient quantity than $p_{k\to n}$ because $p_{k\to n}$ depends explicitly on a numerical parameter, the time step, whereas $P_k(t_0, t)$ depends only on a physical parameter.

To run surface hopping simulations based on the cumulative hopping probability, at the start of a simulation we draw a uniform random number $\eta \in \mathcal{U}(0, 1)$ and hops occur at times when the cumulative probability crosses the random number,

$$P_k(t_0, t^{\text{hop}}) = \eta. \tag{15}$$

$P_k(t_0, t)$ is propagated in time according to

$$P_k(t_0, t + \Delta t) = P_k(t_0, t) + (1 - P_k(t_0, t))\,(1 - e^{-g_k \Delta t}). \tag{16}$$

See the Appendix for a derivation of Eqs. (16-14). We emphasize that Eq. (12) is a special case of Eq. (16) when $t_0 = t$, providing further evidence that Eq. (12) is the correct hopping probability to

use. One random number is drawn and one cumulative probability is integrated irrespective of the number of electronic states. When a hop is indicated by Eq. (15), then the target state for hopping, k', is chosen randomly according to the instantaneous hopping probabilities, $g_{k\to n}(t)$. Note, for two-state models, this step can be ignored. Next, the cumulative probability, P_k, is reset to zero and a new random number is drawn. The cumulative probabilities are reset also in the case of frustrated hops.

The total number of random numbers drawn over the course of a trajectory is thus $\min(2, N_{\text{states}}-1)(N_{\text{hops}}+1)$, which is importantly independent of any purely numerical parameters. We refer to this scheme as FSSH with cumulative probabilities (FSSH-c) and it is compared schematically to FSSH-i in Fig. 1.

C. Even Sampling FSSH (ES-FSSH)

FSSH-c, introduced in the previous section, remains a fully stochastic algorithm to simulate nonadiabatic dynamics through FSSH. In this section, we introduce a semistochastic algorithm for FSSH, called even sampling FSSH (ES-FSSH) that follows directly from the FSSH-c framework. In short, rather than randomly choosing a set of $\{\eta\}$ (and thus the hopping times) for each trajectory, a swarm of trajectories with predetermined values of $\{\eta\}$ is initiated.

We motivate the discussion of ES-FSSH by writing an expectation value over a swarm of FSSH-c simulations with identical initial conditions, $\langle A\rangle$, as the integral expression

$$\langle A\rangle = \int_0^1 dp_1 \int_0^1 dp_2 \ldots \times A(p_1, p_2, \ldots), \tag{17}$$

where $A(p_1, p_2, \ldots)$ is the result obtained from a simulation with $\{\eta\} = \{p_1, p_2, \ldots\}$. In this context, FSSH-c can be seen as a Monte Carlo integration of Eq. (17). The infinitely nested integral above can be tamed by defining reduced expectation operators,

$$A_k(p_1, \ldots, p_k) = \int_0^1 dp_{k+1} \int_0^1 dp_{k+2} \ldots \times A(p_1, \ldots, p_k, p_{k+1}, \ldots) \tag{18}$$

and rewriting Eq. (17) as

$$\langle A \rangle = \int A_1(p_1) dp_1 \tag{19a}$$

$$= \iint A_2(p_1, p_2) dp_1 dp_2 \tag{19b}$$

$$= \iiint A_3(p_1, p_2, p_3) dp_1 dp_2 dp_3. \tag{19c}$$

In essence, ES-FSSH directly computes the expectation value by integrating (19) with an integration quadrature while integrating A_k with a Monte Carlo algorithm, i.e.,

$$\langle A \rangle \approx \sum_i w_i A_1(p_i) \tag{20a}$$

$$\approx \sum_{i,j} w_i w_j A_2(p_i, p_j) \tag{20b}$$

$$\approx \sum_{i,j,k} w_i w_j w_k A_3(p_i, p_j, p_k), \tag{20c}$$

where $\{(w_i, p_i)\}$ are the weights and nodes of an integration rule.

With identical initial conditions, any two trajectories will be identical up until the first hop at which they differ and thus running them as independent trajectories is computationally wasteful. In our implementation, a single trajectory is launched and new trajectories are "spawned" whenever a hopping threshold is crossed. In this way, only the unique portion of trajectories are propagated. For $N_{\text{states}} > 2$, one new trajectory is spawned for each potential target state and the newly spawned trajectories are weighted by the instantaneous probability of hopping.

ES-FSSH is conceptually similar to the accelerated semiclassical Monte Carlo (A-SCMC) method[44], in which for a given set of initial conditions the molecular wavefunction is expanded in terms of an infinite integral over the number and times of hops. The wavefunction for a finite number of hops was built by restarting previously run trajectories with additional hops. For example, A-SCMC is initiated with a single trajectory with no hops, then a 1D spline is generated for all the wavefunction parameters as a function of time, and finally new trajectories are sampled from the 1D splined parameters. In contrast to A-SCMC, ES-FSSH does not require precomputing any trajectories. For example, A-SCMC requires a complete zero-hop trajectory in order to sample single-hop trajectories, whereas ES-FSSH does not. Therefore, ES-FSSH is compatible with a completely on-the-fly approach. Similarly, ES-FSSH resembles full multiple spawning (FMS)[38] in that new trajectories are initiated as needed by spawning from an active trajectory. Both methods reduce the computational cost by initiating a single trajectory and spawning new trajectories only

as needed. They differ in that the collection of ES-FSSH trajectories approximates a swarm of independent trajectories whereas all FMS trajectories are used to expand a single nuclear-electronic time-dependent wavefunction. In addition, with ES-FSSH the total number of trajectories is directly specified by the choice of the quadrature whereas the total number of trajectories is specified indirectly in FMS by a spawning threshold that can lead to exponential growth in the number of trajectories.

III. RESULTS

All of the above algorithms were implemented in mudslide[47], an open source python package for nonadiabatic molecular dynamics. All results use mudslide version 0.9, which is released under the MIT open source license. In mudslide, the classical nuclear equation of motion is propagated using the velocity Verlet algorithm and the quantum electronic problem is propagated as a density matrix by constructing the time-evolution operator using a matrix exponential of $\bar{\mathbf{H}}$. All surface hopping simulations were performed in the adiabatic representation.

For concreteness, we focus on results from two previously published models, Tully's simple avoided crossing model[24] and Prezhdo's superexchange model.[30] We argue that these two models are sufficient, because our aim is to show that FSSH-c is *identical* to FSSH-i, not to survey the performance of FSSH.

Tully's simple avoided crossing. The simple avoided crossing model is a single-particle two-state model designed to mimic a scattering event in which the particle has mass 2000 a.u. and the diabatic Hamiltonian,

$$\mathbf{H}(x) = \begin{pmatrix} V_{11}(x) & V_{12}(x) \\ V_{21}(x) & V_{22}(x) \end{pmatrix}, \tag{21}$$

is defined through

$$V_{11}(x) = \mathrm{sgn}(x) A \left(1 - e^{-B|x|}\right), \tag{22a}$$

$$V_{22}(x) = -V_{11}(x), \tag{22b}$$

$$V_{12}(x) = V_{21}(x) = C e^{-Dx^2}, \tag{22c}$$

where $\mathrm{sgn}(x)$ is the sign function that returns ± 1, $A = 0.01$, $B = 1.6$, $C = 0.005$, and $D = 1.0$, all in atomic units. See Fig. 2a for a depiction of the potential energy surfaces of the simple avoided crossing model.

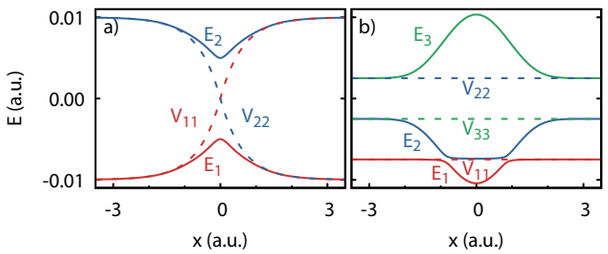

FIG. 2. Nonadiabatic models used in this paper. a) Tully's simple avoided crossing model.[24] b) Prezhdo's super exchange model (note: each energy has been shifted down by 0.0075 a.u. to put it in the same scale).[30]

Prezhdo's superexchange. The superexchange model is a single-particle three-state model designed to mimic mediated electronic processes (i.e., superexchange) in which the particle has mass 2000 a.u. and the diabatic Hamiltonian,

$$\mathbf{H}(x) = \begin{pmatrix} V_{11}(x) & V_{12}(x) & 0 \\ V_{21}(x) & V_{22}(x) & V_{23}(x) \\ 0 & V_{32}(x) & V_{33}(x) \end{pmatrix}, \tag{23}$$

is defined through

$$V_{11}(x) = 0, \tag{24a}$$
$$V_{22}(x) = 2A, \tag{24b}$$
$$V_{33}(x) = A, \tag{24c}$$
$$V_{12}(x) = V_{21}(x) = Be^{-Dx^2}, \tag{24d}$$
$$V_{23}(x) = V_{32}(x) = Ce^{-Dx^2}, \tag{24e}$$

where $A = 0.005$, $B = 0.001$, $C = 0.01$, and $D = 0.5$, all in atomic units. See Fig. 2b for a depiction of the potential energy surfaces of the simple avoided crossing model.

A. FSSH-i and FSSH-c are equivalent

We start by demonstrating numerically that FSSH-i and FSSH-c reproduce the same dynamics. However, the equivalence of FSSH-i and FSSH-c can only be established in the statistical sense, since direct comparisons between trajectories is not possible, i.e., even with the same sequence of random numbers, FSSH-i and FSSH-c trajectories will be distinct.

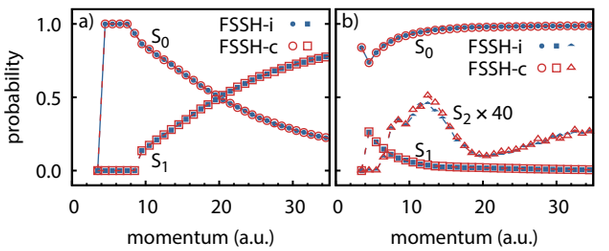

FIG. 3. Transmission probabilities from scattering simulations using FSSH-c (red, open) and FSSH-i (blue, filled) on a) Tully's simple avoided crossing model[24] and b) Prezhdo's super exchange model.[30] Averaged results computed from 10^5 independent trajectories.

For each diabatic model and for both algorithms, we simulated the branching ratio of the scattering event (i.e., the probability of ending the simulation on each electronic surface) as a function of the initial momentum, k_0. For each set of simulations, trajectories were initiated with initial position $x_0 = -10$ a.u. and propagated with time step $\Delta t = \frac{15 \text{ a.u.}}{k_0} \times$ a.u. Statistical properties were computed using 10^5 trajectories for both FSSH-c and FSSH-i. Fig. 3 shows that results simulated using FSSH-i and FSSH-c are visually indistinguishable.

Next, we quantify the equivalence of the two approaches by modeling the final result of each trajectory as a Bernoulli process where the two possible outcomes are ending on the ground state (with associated probability p) or on the excited state (with probability $1 - p$). According to the central limit theorem, with sufficient sampling, the probability distribution for the true branching probability for a given set of initial conditions will follow a normal distribution,

$$\mathcal{P}(p) = \frac{1}{\sigma_p \sqrt{2\pi}} \exp\left(-\frac{1}{2}\left(\frac{p - \bar{p}}{\sigma_p}\right)^2\right), \tag{25}$$

where $\bar{p}$ is the observed mean branching probability, $\sigma_p = \sqrt{\bar{p}(1-\bar{p})/N_\text{s}}$ is the standard error of the mean,[48] and N_s is the number of samples (i.e., independent trajectories). Applying this model for results from FSSH-i and FSSH-c, we can estimate the probability that the true means computed from FSSH-i and FSSH-c differ by less than a tolerance, r, as

$$\mathcal{E}(r) = \frac{1}{2}\left[\text{erf}\left(\frac{\Delta\bar{p} + r}{\sqrt{2}\sigma'}\right) - \text{erf}\left(\frac{\Delta\bar{p} - r}{\sqrt{2}\sigma'}\right)\right], \tag{26}$$

where $\text{erf}(x)$ is the error function, $\Delta\bar{p}$ is the difference between the observed branching probabilities for FSSH-i and FSSH-c, and $\sigma' = \sqrt{\sigma^2_{\text{FSSH-i}} + \sigma^2_{\text{FSSH-c}}}$ is the combined standard error of the mean for FSSH-i and FSSH-c.

Using Eq. (26), we find that branching probabilities computed with FSSH-i and FSSH-c differ by less than 0.011 at 99% confidence for all initial momenta in Fig. 3. Consequently, we confirm that FSSH-i and FSSH-c produce statistically identical results. In other words, any swarm FSSH-c trajectories will exhibit the exact same statistical properties (e.g., mean and variance) as a swarm of FSSH-i trajectories, regardless of the model or number of trajectories in the swarms.

An important caveat is that FSSH-i and FSSH-c produce identical results *for sufficiently small time steps*. For larger time steps, we found a small but statistically significant difference between FSSH-i and FSSH-c when the hopping probability becomes large. Figure 4a shows the results of sets of 10^5 scattering simulations with the same parameters as in Fig. 3, except with a time step of $\Delta t = \frac{120 \text{ a.u.}}{k_0} \times$ a.u, which is 8 times larger than that used in Fig. 3. We see that when the initial momentum becomes large (and the probability of ending the simulation on the excited state increases), there is a small but systematic difference between FSSH-c and FSSH-i, with FSSH-i being more likely to end on the excited state. Since the only difference between the two algorithms is in the hopping decision, we conclude that the difference between FSSH-i and FSSH-c in Fig. 4 is due to overly aggressive hopping in the FSSH-i algorithm. We verified by investigating the convergence with respect to time step for a set of simulations with initial momentum $k_0 = 30$ a.u. and averaged over 10^6 trajectories, and further comparing against FSSH-ip (FSSH-i with scaled Poisson probabilities). The results are shown in Fig. 4b, from which we see that FSSH-c and FSSH-ip have similar convergence rates and that FSSH-i requires a significantly shorter time step than FSSH-c for the same accuracy; FSSH-c and FSSH-ip are essentially converged by $\Delta t = 4$ a.u. (i.e., the difference between the result at $\Delta t = 4$ a.u. is within one standard deviation of the result at $\Delta t = \frac{1}{4}$ a.u.), whereas FSSH-i requires a time step of $\Delta t = \frac{1}{2}$ a.u. for the result to be within one standard deviation of the result at $\Delta t = \frac{1}{4}$ a.u. For instance, the FSSH-i result with $\Delta t = 1$ a.u. is more than 4 standard deviations away from the result with $\Delta t = \frac{1}{4}$ a.u.

B. FSSH-c uncovers convergence behavior

In this section, we demonstrate the key advantage of FSSH-c: it enables detailed investigations of the convergence behavior of a *single trajectory* with respect to any other numerical parameter such as the time step, integration method, or thresholds related to construction of the potential energy surfaces. This is not possible using FSSH-i because changing the time step will necessarily change the sequence of random numbers drawn for a given physical time interval. Hence,

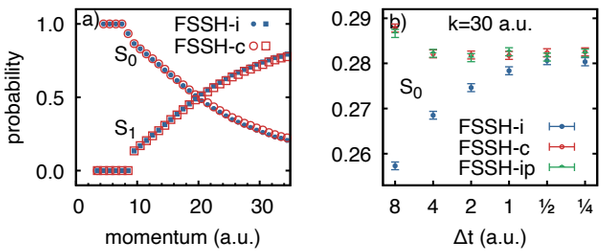

FIG. 4. a) Transmission probabilities from scattering simulations on Tully's simple avoided crossing model[24] using FSSH-c (red, open) and FSSH-i (blue, filled) with $\Delta t = \frac{120\text{ a.u.}}{k_0} \times$ a.u, which is 8 times larger than time steps used in Fig. 3. b) Convergence of the probability of transmission on the ground state with initial momentum $k_0 = 30$ a.u. as a function of time step. Averaged results computed from 10^5 independent trajectories. Vertical bars represent the 95% confidence interval estimated from $\pm 1.96\sqrt{p(1-p)/N_s}$ where p is the observed ground state transmission probability and $N_s = 10^6$.

convergence studies for *single surface hopping trajectories* have not been reported previously.

The convergence of the final position, momentum, energy, and density matrix as well as the hopping times of a single trajectory with respect to time step is examined in Fig. 5. The trajectory uses Tully's simple avoided crossing model, with initial position $x_0 = -10$ a.u., initial momentum $k_0 = 10.0$ a.u., and initial density matrix $\sigma_{nm}(0) = \delta_{0n}\delta_{0m}$. Trajectories were run for a total time of 4000 a.u. As reference, we compare to a trajectory with $\Delta t = 2^{-14}$ a.u. $\approx 6.1 \times 10^{-5}$ a.u. In the studied trajectories, two hops are observed such that three random numbers are generated with values of {0.0291974618580323, 0.1800264840275190, 0.2221643371943814}.

From Fig. 5, we see that all final parameters converge monotonically and that a parts-per-thousand error is achieved for most final properties at $\Delta t = 1$ a.u. Notably, most properties converge much slower than expected analytically. For instance, the analytical global error in the position for the velocity Verlet algorithm scales as Δt^2; however, a log-log fit of the results in Fig. 5a show a scaling of $\Delta t^{0.98}$. We attribute this slow convergence to the result of surface hops. The error in the hopping time is linear in the time step, because hops are only considered at whole time steps. Because the potential energy surface and momentum change suddenly upon surface hop, a linear error in the hopping time translates into a linear error in all other properties. We corroborated this hypothesis by studying the convergence of a trajectory with no hops and find that the position, energy, momentum, and magnitudes of all elements of the density matrix converge quadratically or faster.

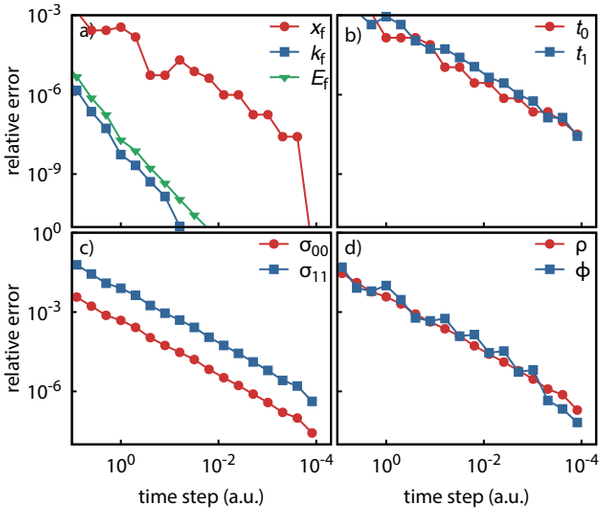

FIG. 5. Convergence of a single surface hopping trajectory with respect to time step using FSSH-c. Relative errors of the final a) position (x_f), momentum (k_f), and total energy (E_f); b) time of first surface hop (t_0) and second surface hop (t_1); c) diagonal elements of the electronic density matrix ($\sigma_{00}(t_f)$ and $\sigma_{11}(t_f)$); d) off-diagonal elements of the electronic density matrix in polar form, $\sigma_{01}(t_f) = \rho e^{i\phi}$.

C. ES-FSSH reduces statistical error but biases the results

In this section, we compare statistical convergence of FSSH-c with several closely related even sampling FSSH (ES-FSSH) methods. In all cases, we use the trapezoid rule to integrate Eq. (19). We also tested integration based on Simpson's rule but found no systematic difference. See the supplementary material for results using Simpson's rule integration.[49] We further introduce the ESn family of even sampling algorithms in which an n-dimensional quadrature is used to integrate A_n in Eq. (19). We denote ESn(w,m) algorithm as the even sampling algorithm with w quadrature points in each dimension integrating A_n and m Monte Carlo samples for each value of A_n. ESn(w, m) thus uses mw^n trajectories to approximate $\langle A \rangle$. For instance, ES1(10,5) approximates Eq. (19) by integrating $A_1(p)$ with a 10-point midpoint integration rule where each value of $A_1(p)$ is computed by averaging across 5 independent trajectories.

Figure 6 compares the expected means and 95% confidence intervals obtained from FSSH-c, ES1, ES2, and ES3 with different values of w and m for a scattering simulation using Tully's simple avoided crossing with initial position $x_0 = -10$ a.u., initial momentum $k_0 = 10$ a.u., and initial density matrix $\sigma_{nm}(0) = \delta_{0n}\delta_{0m}$. A time step of $\Delta t = 1.0$ a.u. was used. The expected mean

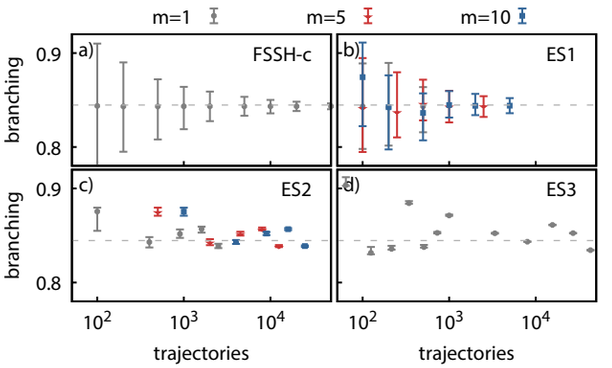

FIG. 6. Comparison of statistical convergence of a) FSSH-c and even sampling algorithms b) ES1, c) ES2, and d) ES3 on Tully's simple avoided crossing model. Points signify the mean and vertical bars the 95% confidence interval of a set of trajectories. For ES1, values of $w = 10, 20, 50, 100, 200, 500, 1000$ were used. For ES2, values of $w = 10, 20, 30, 40, 50$ were used. For ES3, values of $w = 3, 4, 5, 7, 8, 9, 10, 15, 20, 25, 30, 35$ were used. The horizontal dashed line shows the mean obtained by averaging 10^6 trajectories. Computational savings from reusing large portions of trajectories in ESn algorithms are not include in this plot.

and confidence intervals for FSSH-c were obtained by bootstrap sampling on a collection of 10^6 independent trajectories, while the expected mean and confidence intervals for ESn were obtained by repeating the ESn simulation 100 times.

As expected from a Monte Carlo integration, FSSH-c is unbiased but relatively slow to converge; the mean branching probability, 0.843, is numerically identical to the mean computed using 10^6 samples, but the range of the 95% confidence interval scales as $N_s^{-0.49}$. The ESn algorithms, on the other hand, effectively trade bias for faster statistical convergence. Furthermore, we find that increasing the value of m, i.e., the number of Monte Carlo samples, reduces the range of the confidence interval but does not change the expected mean. For this reason, increased sampling with m is only beneficial in the ES1 scheme, where the bias is small but the statistical noise is significant. For concreteness, consider the ES2 results shown in Fig. 6c. The branching probability computed using ES2(10,1)—which spawns 100 trajectories in total—has a mean of 0.875 with a 95% confidence interval 0.855–0.880 and root-mean-square-error (RSME) of 0.033, compared to a mean of 0.843 with a 95% confidence interval 0.770–0.910 and RMSE of 0.037 obtained using FSSH-c with 100 trajectories. Therefore, a "typical" result using ES2(10,1) is closer to the converged result than a "typical" result computed with 100 FSSH-c trajectories, even though the *average* result from a large number of repeated simulations with ES2(10,1) will not converge to

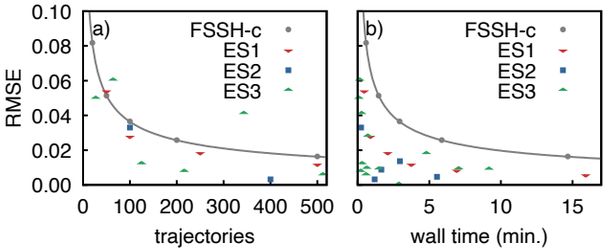

FIG. 7. Comparison of root-mean-square-error (RMSE) of FSSH-c and even sampling algorithms as a function of a) the number of trajectories and b) the wall time required. The solid line shows the analytical RMSE for independent FSSH-c trajectories and points show the observed numerical results for all methods presented in Fig. 6. ES1 uses $m = 5$, while ES2 and ES3 use $m = 1$ Monte Carlo samples. RMSE for FSSH-c estimated from bootstrap sampling, and by 100 repeated simulations for ESn.

the same limit as a large number of FSSH-c trajectories. No significant benefit is gained from the ES2(10,5) scheme, which reduces the RMSE only to 0.032. On the other hand, when going from ES1(50,1) to ES1(50,10), the RMSE is reduced from 0.040 to 0.014 while the computational time increases by a factor of 9.

A more direct comparison of ES-FSSH with FSSH-c is shown in Fig. 7 in which we compare the expected error in terms of the RMSE of a set of FSSH-c or ESn simulations as a function of the number of trajectories or the wall time required for the simulations. We restrict our attention in Fig. 7 to swarms with fewer than 500 trajectories to better reflect the most common use cases of FSSH with ab initio potentials, and we use $m = 5$ for ES1 and $m = 1$ for ES2 and ES3. The RMSE results are obtained from bootstrap sampling for FSSH-c and from 100 repeated simulations for ESn. In Fig. 7a we see that ESn is competitive with FSSH-c on a per trajectory comparison, with some ESn algorithms outperforming FSSH-c and a few widely underperforming. ES1 in particular, reduces the number of trajectories needed for a given accuracy by factors of 1.7, 1.5, and 1.8 for $w = 20$, 50, and 100, respectively. However, the comparison in terms of number of trajectories neglects the significant computational savings gained by only simulating the unique portions of trajectories. Fig. 7b shows the same results but as a function of the wall time required for the simulations. Here, we see that even the worst performing ESn algorithms require approximately a quarter as much wall time to achieve the same RMSE as FSSH-c, while top performing ESn algorithms (especially ES3) achieve accuracies which could only be attained from tens of thousands of FSSH-c trajectories at a small fraction of the cost.

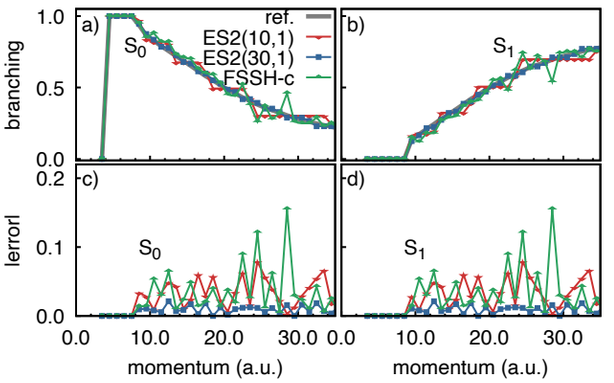

FIG. 8. Comparison of ES2(10,1), ES2(30,1), and 100 FSSH-c trajectories on Tully's simple avoided crossing model. Reference results are taken from the 10^5 trajectories shown in Fig. 3. a) Probability of remaining on the ground electronic state and c) the error relative to converged results. b) Probability of transitioning to the excited electronic state and d) the error relative to converged results.

To test whether the performance of ES-FSSH generalizes beyond the single momentum investigated in Fig. 6, we compute the branching probabilities as a function of initial momentum, k_0, using ES2(10,1), ES2(30,1), and 100 FSSH-c trajectories. The results are collected in Fig. 8 and compared to the reference results obtained in Fig. 3. All other simulation parameters are the same for the results shown in Fig. 3, i.e., $x_0 = -10$ a.u., $\Delta t = \frac{15 \text{ a.u.}}{k_0} \times$ a.u. In Fig. 8, we see that all 3 methods closely track the reference results, but that 100 FSSH-c trajectories show the largest maximum error and are notably nonmonotonic, whereas both sets of ES2 results recover the monotonic behavior of the reference result. In addition, the ES2(30,1) results are closest to the reference results at all momenta.

We conclude this section by noting that electronic state branching probabilities for this model are likely a "worst case" model for the ESn because the branching probability is directly related to the number of hops and ESn treats the n-th hop differently than the $n+1$ hop. For example, in ES2, the first two hops are included in the quadrature while the third is recovered through Monte Carlo sampling of A_2. However, for many applications of FSSH in chemistry, the final electronic state is known and FSSH is used to estimate not how many hops will occur but *when* and *how* they will occur. For example, in photodeactivation simulations, such as the deactivation of photoexcited thymine,[21] nearly every trajectory undergoes the same number and sequence of hops.

IV. CONCLUSIONS

Here, we introduce a cumulative approach to fewest switches surface hopping (FSSH-c) in which surface hops are initiated when the cumulative hopping probability crosses a random number, instead of the conventional prescription in which hops occur when the instantaneous conditional probability is greater than a random number (FSSH-i). Importantly, FSSH-c produces statistically identical results as the conventional FSSH algorithm, and is thus an interchangeable replacement. As a byproduct, we show that FSSH-i overestimates the hopping probability when the instantaneous probability becomes large and propose a simple scaling fix that improves convergence with respect to time step. FSSH-c shares the same algorithmic structure as FSSH-i, and requires only a single additional floating point scalar variable to be retained between time steps—the cumulative hopping probability. Existing FSSH-i implementations can be converted to FSSH-c implementations with trivial modification of existing routines.

The key feature of FSSH-c is that surface hops are independent of numerical parameters such as the time step. By removing the dependence of surface hops on the time step, several new possibilities are opened up, two of which are explored here. First, the convergence behavior of *single trajectories* with respect to time step can be studied numerically. Our results indicate that the leading error in surface hopping simulations appears to scale linearly with time step, whereas a quadratic global error is expected analytically for the velocity Verlet method. The loss of accuracy in the surface hopping simulations shown here likely result from the choice to only allow hops to occur at the discrete times dictated by time step. Therefore, we conclude that algorithms that allow surface hops to occur at a continuous time within a time step hold great promise for improving the numerical accuracy of surface hopping simulations.

Second, FSSH-c exposes an alternative semistochastic integration technique for surface hopping simulations which accelerates convergence at the expense of bias, that we call even sampling FSSH (ES-FSSH). In particular, we introduced the ESn family of ES-FSSH algorithms which integrate the first n hops in a swarm of simulations with an integration quadrature and all further hops with a Monte Carlo integration. For low numbers of trajectories (≈ 100), ESn appears advantageous because the bias introduced by the quadrature is significantly smaller than the statistical variance of the Monte Carlo approach. We emphasize that the example shown above is likely a worst-case scenario for ESn. In contrast to similar algorithms to approximate swarms of FSSH trajectories, ESn is fully compatible with on-the-fly dynamics[44] and does not require manual se-

lection of coupling thresholds.[35]

Finally, FSSH-c has significant advantages over FSSH-i in terms of reproducibility and comparability of different implementations. For example, directly comparing two different FSSH-i implementations requires using identical random number generators and time steps at the least, meaning that algorithms implemented in different languages (with different random number libraries) may be impossible to directly compare. In this paper, we needed 10^5 trajectories to have a 99% confidence that branching ratios computed with FSSH-i and FSSH-c agreed to within 0.011. Because of the slow convergence of Monte Carlo integration, we estimate that approximately 10^7 trajectories would be required to tighten the window of agreement to 0.001. By contrast, two implementations of FSSH-c could be compared to machine precision with just a single trajectory. Thus, FSSH-c significantly reduces the effort required for computational reproduction. Furthermore, since hops only depend on physical characteristics of the trajectories, they should be much less sensitive to details of the integration than in FSSH-i, meaning direct comparison is simple even between methods that use different integration schemes, such as higher-order symplectic integrators[50] or adaptive- or multiple-time stepping.[51]

As our focus here is to show the myriad advantages of working in the cumulative framework, we defer more detailed studies of the convergence and stability of propagation algorithms and of the even sampling surface hopping algorithm to future publications. A plethora of extensions can be envisioned. We briefly mention only a few. Surface hopping algorithms that allow surface hops to occur on the interior of time steps have been proposed[52] and can now be systematically evaluated. Different integration quadratures in ES-FSSH could be investigated, including sparse Smolyak grids[41,53,54] and adaptive integration schemes.[55] In particular, we imagine that integration quadratures for even sampling could be matched to the chemical process (e.g., excited-state decay vs intersystem crossing) or specially designed to capture rare events without specifying in advance additional numerical parameters.[35,56] Although we focused on the hopping probability in FSSH, the same approach is applicable to any random process in related algorithms, such as the collapse or reset probabilities in Augmented-FSSH[28,52,57] or tunneling events in classical trajectories.[58] All of these directions are under investigation on our group.

FSSH-c has significant advantages over FSSH-i, no discernible disadvantages, and a trivial implementation. Therefore, we recommend its adoption as default in all FSSH implementations.

SUPPLEMENTARY MATERIALS

See the supplementary materials for even sampling fewest switches surface hopping results integrated using Simpson's rule.

ACKNOWLEDGMENTS

This work was supported by a startup fund from CWRU. C.J.S. was supported by a SOURCE fellowship from CWRU. This work made use of the High Performance Computing Resource in the Core Facility for Advanced Research Computing at Case Western Reserve University.

DATA AVAILABILITY

The data that support the findings of this study are openly available in "Surface hopping with cumulative probabilities: even sampling and improved reproducibility" at http://doi.org/10.17605/OSF.IO/73PW4.

Appendix: Propagation of Cumulative Probability

In this section, we derive the propagation of the cumulative probability of hopping out of state k, $P_k(t_0, t)$, which represents the total probability of a single hop occurring between t_0 and t. For convenience, however, we work with the probability of finding *no* hops in the interval, $\bar{P}_k(t_0, t) \equiv 1 - P_k(t_0, t)$ for the duration of the derivation and rewrite the final result in terms of $P_k(t_0, t)$. Our implementation propagates $P_k(t_0, t)$. We start by writing the infinitesimal change as

$$\bar{P}_k(t_0, t + dt) = \bar{P}_k(t_0, t)\,(1 - G_k(t)) \tag{A.1}$$

where the term on the right side represents the probability of there being no hop in the interval (t_0, t) *and* no hop in $(t, t + dt)$, and

$$G_k(t) = 1 - \prod_{n \neq k} (1 - H(g_{k\to n}(t))dt) \tag{A.2}$$

is the total probability of a hop to any state in the time interval. In the previous equation, $H(x)$ is the Heaviside function which ensures the result is nonnegative. Expanding $G_k(t)$ and discarding

terms quadratic and higher in dt we find that $G_k(t) = g_k(t)dt$, where

$$g_k(t) = \sum_{n \neq k} H(g_{k\to n}(t)). \tag{A.3}$$

Eq. (A.1) can be transformed into the differential equation,

$$\frac{d\bar{P}_k}{dt} = -g_k(t)\bar{P}_k(t_0, t). \tag{A.4}$$

Integrating the previous equation to determine $\bar{P}_k(t_0, t + \Delta t)$ for some finite time step Δt, we find

$$\bar{P}_k(t_0, t + \Delta t) = \bar{P}_k(t_0, t) \exp\left(-\int_t^{t+\Delta t} g_k(t')dt'\right). \tag{A.5}$$

We arrive at Eq. (16) by assuming $g_k(t)$ is constant in the interval from $(t, t + \Delta t)$ and rewriting in terms of $P_k(t_0, t + \Delta t)$,

$$P_k(t_0, t + \Delta t) = 1 - (1 - P_k(t_0, t))\, e^{-g_k \Delta t} \tag{A.6a}$$

$$= P_k(t_0, t) + (1 - P_k(t_0, t))\,(1 - e^{-g_k \Delta t}). \tag{A.6b}$$

For improved numerical stability, our implementation uses the form in Eq. (A.6b) with the expm1 routine in numpy[59] to directly compute $e^{-g_k\Delta t} - 1$, which has greater numerical precision for small arguments. Similar functions are available in C and C++.

We close this section by noting that Eq. (A.5), which is exact for any $g_k(t)$, exposes an alternative strategy in which hops occur when

$$\int_{t_0}^{t^{\text{hop}}} g_k(t')dt' = \ln\left(\frac{1}{1-\eta}\right), \tag{A.7}$$

rather than the condition used in this paper.

REFERENCES

[1]Barbatti, M. Nonadiabatic Dynamics with Trajectory Surface Hopping Method. *WIREs Comput. Mol. Sci.* **2011**, *1*, 620–633.

[2]Agostini, F.; Curchod, B. F. E. Different Flavors of Nonadiabatic Molecular Dynamics. *WIREs Comput. Mol. Sci.* **2019**, *9*, e1417.

[3]Smith, B.; Akimov, A. V. Modeling Nonadiabatic Dynamics in Condensed Matter Materials: Some Recent Advances and Applications. *J. Phys.: Condens. Matter* **2019**, *32*, 073001.

[4]Curchod, B. F. E.; Sisto, A.; Martínez, T. J. Ab Initio Multiple Spawning Photochemical Dynamics of DMABN Using GPUs. *J. Phys. Chem. A* **2017**, acs.jpca.6b09962.

[5]Shenvi, N.; Roy, S.; Tully, J. C. Nonadiabatic Dynamics at Metal Surfaces: Independent-Electron Surface Hopping. *J. Chem. Phys.* **2009**, *130*, 174107.

[6]Dou, W.; Subotnik, J. E. Nonadiabatic Molecular Dynamics at Metal Surfaces. *J. Phys. Chem. A* **2020**, *124*, 757–771.

[7]Fiedlschuster, T.; Handt, J.; Schmidt, R. Floquet Surface Hopping: Laser-Driven Dissociation and Ionization Dynamics of H$_{2}{\hat}{+}$. *Phys. Rev. A* **2016**, *93*, 053409.

[8]Hoffmann, N. M.; Schäfer, C.; Säkkinen, N.; Rubio, A.; Appel, H.; Kelly, A. Benchmarking Semiclassical and Perturbative Methods for Real-Time Simulations of Cavity-Bound Emission and Interference. *J. Chem. Phys.* **2019**, *151*, 244113.

[9]Pérez-Sánchez, J. B.; Yuen-Zhou, J. Polariton Assisted Down-Conversion of Photons via Nonadiabatic Molecular Dynamics: A Molecular Dynamical Casimir Effect. *J. Phys. Chem. Lett.* **2020**, *11*, 152–159.

[10]Craig, C. F.; Duncan, W. R.; Prezhdo, O. V. Trajectory Surface Hopping in the Time-Dependent Kohn-Sham Approach for Electron-Nuclear Dynamics. *Phys. Rev. Lett.* **2005**, *95*, 163001.

[11]Tapavicza, E.; Tavernelli, I.; Rothlisberger, U. Trajectory Surface Hopping within Linear Response Time-Dependent Density-Functional Theory. *Phys. Rev. Lett.* **2007**, *98*, 023001.

[12]Tapavicza, E.; Tavernelli, I.; Rothlisberger, U.; Filippi, C.; Casida, M. E. Mixed Time-Dependent Density-Functional Theory/Classical Trajectory Surface Hopping Study of Oxirane Photochemistry. *J. Chem. Phys.* **2008**, *129*, 124108.

[13]Fischer, S. A.; Habenicht, B. F.; Madrid, A. B.; Duncan, W. R.; Prezhdo, O. V. Regarding the Validity of the Time-Dependent Kohn–Sham Approach for Electron-Nuclear Dynamics via Trajectory Surface Hopping. *J. Chem. Phys.* **2011**, *134*, 024102.

[14]Tavernelli, I.; Curchod, B. F. E.; Rothlisberger, U. Nonadiabatic Molecular Dynamics with Solvent Effects: A LR-TDDFT QM/MM Study of Ruthenium (II) Tris (Bipyridine) in Water. *Chemical Physics* **2011**, *391*, 101–109.

[15]Plasser, F.; Crespo-Otero, R.; Pederzoli, M.; Pittner, J.; Lischka, H.; Barbatti, M. Surface Hopping Dynamics with Correlated Single-Reference Methods: 9H-Adenine as a Case Study. *J. Chem. Theory Comput.* **2014**, *10*, 1395–1405.

[16]Xia, S.-H.; Xie, B.-B.; Fang, Q.; Cui, G.; Thiel, W. Excited-State Intramolecular Proton Transfer to Carbon Atoms: Nonadiabatic Surface-Hopping Dynamics Simulations. *Phys. Chem. Chem.*

Phys. **2015**, *17*, 9687–9697.

[17]Barbatti, M.; Crespo-Otero, R. In *Density-Functional Methods for Excited States*; Ferré, N., Filatov, M., Huix-Rotllant, M., Eds.; Topics in Current Chemistry; Springer International Publishing: Cham, 2016; pp 415–444.

[18]Atkins, A. J.; González, L. Trajectory Surface-Hopping Dynamics Including Intersystem Crossing in [Ru(Bpy)3]2+. *J. Phys. Chem. Lett.* **2017**, *8*, 3840–3845.

[19]Muuronen, M.; Parker, S. M.; Berardo, E.; Le, A.; Zwijnenburg, M. A.; Furche, F. Mechanism of Photocatalytic Water Oxidation on Small TiO2 Nanoparticles. *Chem Sci* **2017**, *8*, 2179–2183.

[20]Yue, L.; Liu, Y.; Zhu, C. Performance of TDDFT with and without Spin-Flip in Trajectory Surface Hopping Dynamics: Cis–Trans Azobenzene Photoisomerization. *Phys. Chem. Chem. Phys.* **2018**, *20*, 24123–24139.

[21]Parker, S. M.; Roy, S.; Furche, F. Multistate Hybrid Time-Dependent Density Functional Theory with Surface Hopping Accurately Captures Ultrafast Thymine Photodeactivation. *Phys. Chem. Chem. Phys.* **2019**, *21*, 18999–19010.

[22]Roy, S.; Ardo, S.; Furche, F. 5-Methoxyquinoline Photobasicity Is Mediated by Water Oxidation. *J. Phys. Chem. A* **2019**, *123*, 6645–6651.

[23]Cao, J.; Chen, D.-c. The Excited-State Relaxation Mechanism of Potential UVA-Activated Phototherapeutic Molecules: Trajectory Surface Hopping Simulations of Both 4-Thiothymine and 2,4-Dithiothymine. *Phys. Chem. Chem. Phys.* **2020**, *22*, 10924–10933.

[24]Tully, J. C. Molecular Dynamics with Electronic Transitions. *J. Chem. Phys.* **1990**, *93*, 1061.

[25]Wang, L.; Akimov, A.; Prezhdo, O. V. Recent Progress in Surface Hopping: 2011–2015. *J. Phys. Chem. Lett.* **2016**, *7*, 2100–2112.

[26]Volobuev, Y. L.; Hack, M. D.; Topaler, M. S.; Truhlar, D. G. Continuous Surface Switching: An Improved Time-Dependent Self-Consistent-Field Method for Nonadiabatic Dynamics. *J. Chem. Phys.* **2000**, *112*, 9716–9726.

[27]Hack, M. D.; Truhlar, D. G. A Natural Decay of Mixing Algorithm for Non-Born–Oppenheimer Trajectories. *J. Chem. Phys.* **2001**, *114*, 9305–9314.

[28]Subotnik, J. E.; Shenvi, N. A New Approach to Decoherence and Momentum Rescaling in the Surface Hopping Algorithm. *J. Chem. Phys.* **2011**, *134*, 024105.

[29]Jaeger, H. M.; Fischer, S.; Prezhdo, O. V. Decoherence-Induced Surface Hopping. *J. Chem. Phys.* **2012**, *137*, 22A545.

[30]Wang, L.; Trivedi, D.; Prezhdo, O. V. Global Flux Surface Hopping Approach for Mixed

Quantum-Classical Dynamics. *J. Chem. Theory Comput.* **2014**, *10*, 3598–3605.

[31]Wang, L.; Sifain, A. E.; Prezhdo, O. V. Communication: Global Flux Surface Hopping in Liouville Space. *J. Chem. Phys.* **2015**, *143*, 191102.

[32]Min, S. K.; Agostini, F.; Gross, E. K. U. Coupled-Trajectory Quantum-Classical Approach to Electronic Decoherence in Nonadiabatic Processes. *Phys. Rev. Lett.* **2015**, *115*, 073001.

[33]Martens, C. C. Surface Hopping by Consensus. *J. Phys. Chem. Lett.* **2016**, *7*, 2610–2615.

[34]Tempelaar, R.; Reichman, D. R. Generalization of Fewest-Switches Surface Hopping for Coherences. *J. Chem. Phys.* **2017**, *148*, 102309.

[35]Nangia, S.; Jasper, A. W.; Miller, T. F.; Truhlar, D. G. Army Ants Algorithm for Rare Event Sampling of Delocalized Nonadiabatic Transitions by Trajectory Surface Hopping and the Estimation of Sampling Errors by the Bootstrap Method. *J. Chem. Phys.* **2004**, *120*, 3586–3597.

[36]Kossoski, F.; Barbatti, M. Nuclear Ensemble Approach with Importance Sampling. *J. Chem. Theory Comput.* **2018**, *14*, 3173–3183.

[37]Preston, R. K.; Tully, J. C. Effects of Surface Crossing in Chemical Reactions: The H3+ System. *J. Chem. Phys.* **1971**, *54*, 4297–4304.

[38]Ben-Nun, M.; Quenneville, J.; Martínez, T. J. Ab Initio Multiple Spawning: Photochemistry from First Principles Quantum Molecular Dynamics. *J. Phys. Chem. A* **2000**, *104*, 5161–5175.

[39]Curchod, B. F. E.; Glover, W. J.; Martínez, T. J. SSAIMS—Stochastic-Selection Ab Initio Multiple Spawning for Efficient Nonadiabatic Molecular Dynamics. *J. Phys. Chem. A* **2020**, *124*, 6133–6143.

[40]National Academies of Sciences, Engineering, and Medicine, *Reproducibility and Replicability in Science*; The National Academies Press: Washington, DC, 2019.

[41]Rodríguez, J. I.; Thompson, D. C.; Ayers, P. W.; Köster, A. M. Numerical Integration of Exchange-Correlation Energies and Potentials Using Transformed Sparse Grids. *J. Chem. Phys.* **2008**, *128*, 224103.

[42]Qiu, J.; Bai, X.; Wang, L. Subspace Surface Hopping with Size-Independent Dynamics. *J. Phys. Chem. Lett.* **2019**, *10*, 637–644.

[43]White, A. J.; Gorshkov, V. N.; Wang, R.; Tretiak, S.; Mozyrsky, D. Semiclassical Monte Carlo: A First Principles Approach to Non-Adiabatic Molecular Dynamics. *J. Chem. Phys.* **2014**, *141*, 184101.

[44]White, A. J.; Gorshkov, V. N.; Tretiak, S.; Mozyrsky, D. Non-Adiabatic Molecular Dynamics by Accelerated Semiclassical Monte Carlo. *J. Chem. Phys.* **2015**, *143*, 014115.

[45]Kapral, R. Progress in the Theory of Mixed Quantum-Classical Dynamics. *Annu. Rev. Phys. Chem.* **2006**, *57*, 129–157.

[46]Wu, Y.; Herman, M. F. A Justification for a Nonadiabatic Surface Hopping Herman-Kluk Semiclassical Initial Value Representation of the Time Evolution Operator. *J. Chem. Phys.* **2006**, *125*, 154116.

[47]mudslide 0.9, available at github.com/smparker/mudslide.

[48]Martin, B. In *Statistics for Physical Science*; Martin, B., Ed.; Academic Press: Boston, 2012; pp 83 – 104.

[49]See Supplementary Material Document No. xxxxx for Even Sampling results integrated using the Simpson rule.

[50]Odell, A.; Delin, A.; Johansson, B.; Bock, N.; Challacombe, M.; Niklasson, A. M. N. Higher-Order Symplectic Integration in Born–Oppenheimer Molecular Dynamics. *J. Chem. Phys.* **2009**, *131*, 244106.

[51]Luehr, N.; Markland, T. E.; Martínez, T. J. Multiple Time Step Integrators in Ab Initio Molecular Dynamics. *J. Chem. Phys.* **2014**, *140*, 084116.

[52]Jain, A.; Alguire, E.; Subotnik, J. E. An Efficient, Augmented Surface Hopping Algorithm That Includes Decoherence for Use in Large-Scale Simulations. *J. Chem. Theory Comput.* **2016**, acs.jctc.6b00673.

[53]Smolyak, S. A. Quadrature and interpolation formulas for tensor products of certain classes of functions. *Dokl Akad Nauk SSSR* **1963**, *148*, 1042–1045.

[54]Avila, G.; Carrington, T. Nonproduct Quadrature Grids for Solving the Vibrational Schrödinger Equation. *J. Chem. Phys.* **2009**, *131*, 174103.

[55]Krack, M.; Köster, A. M. An Adaptive Numerical Integrator for Molecular Integrals. *J. Chem. Phys.* **1998**, *108*, 3226–3234.

[56]Lingerfelt, D. B.; Williams-Young, D. B.; Petrone, A.; Li, X. Direct Ab Initio(Meta-)Surface-Hopping Dynamics. *J. Chem. Theory Comput.* **2016**, acs.jctc.5b00697.

[57]Subotnik, J. E. Fewest-Switches Surface Hopping and Decoherence in Multiple Dimensions. *J. Phys. Chem. A* **2011**, *115*, 12083–12096.

[58]Zheng, J.; Xu, X.; Meana-Pañeda, R.; Truhlar, D. G. Army Ants Tunneling for Classical Simulations. *Chem. Sci.* **2014**, *5*, 2091–2099.

[59]van der Walt, S.; Colbert, S. C.; Varoquaux, G. The NumPy Array: A Structure for Efficient Numerical Computation. *Comput. Sci. Eng.* **2011**, *13*, 22–30.

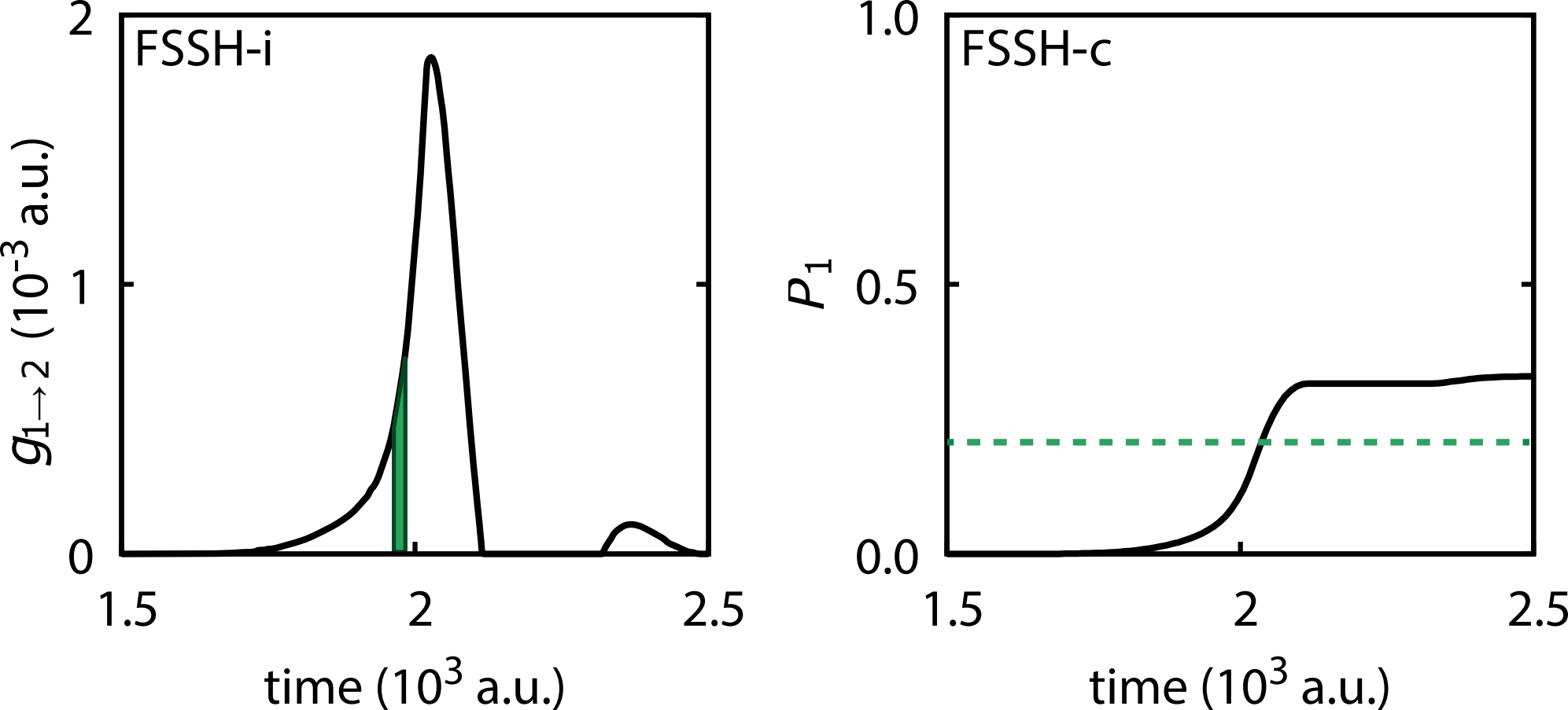
FSSH-i
$g_{1\to 2}$ (10^{-3} a.u.)
2
1
0
1.5
2
2.5
time (10^3 a.u.)
FSSH-c
P_1
1.0
0.5
0.0
1.5
2
2.5
time (10^3 a.u.)

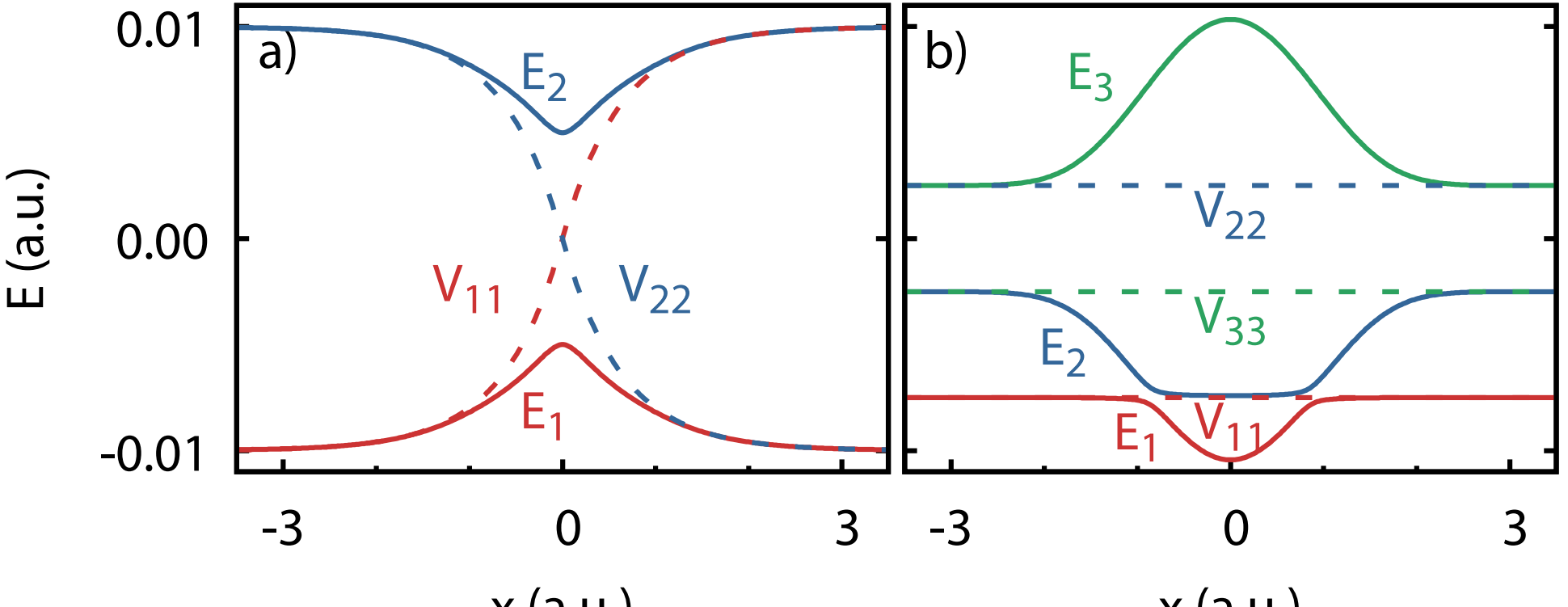
a)
b)
E (a.u.)
0.01
0.00
-0.01
-3
0
3
x (a.u.)
E2
E1
V11
V22
E3
V33

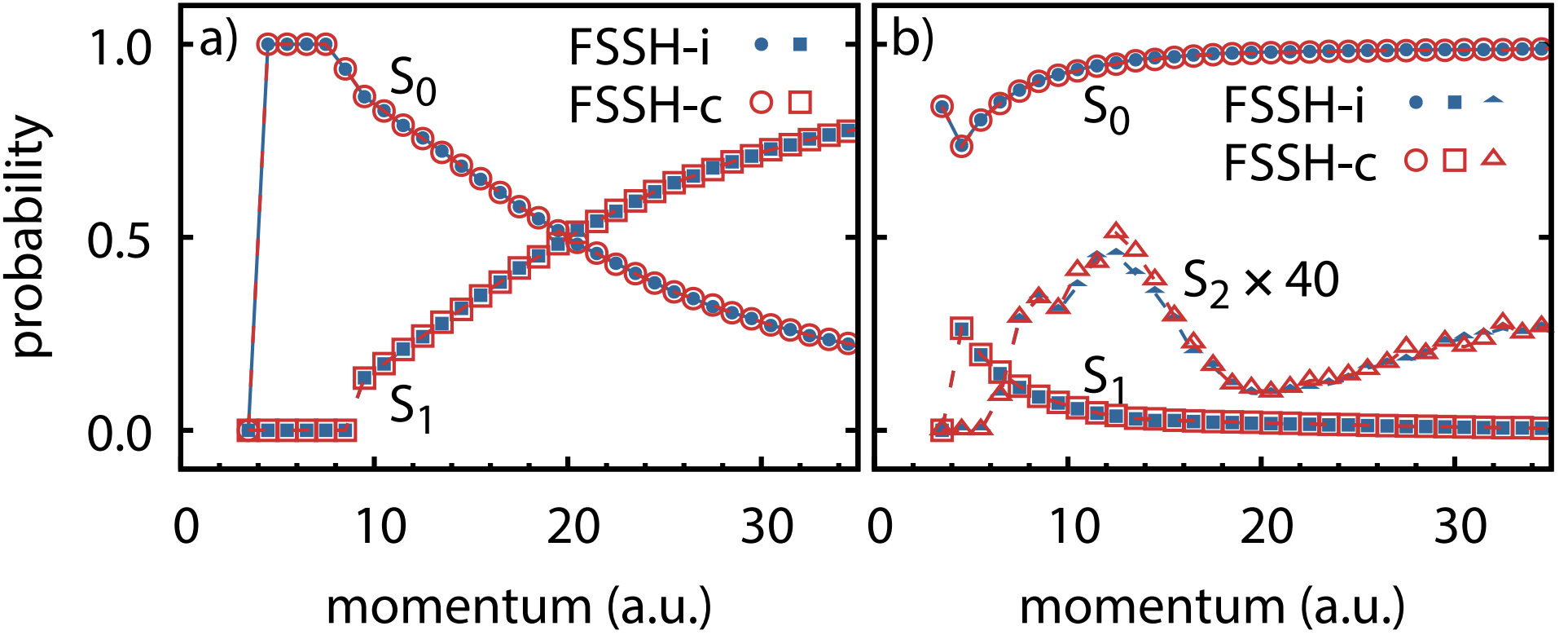
a)
b)
FSSH-i
FSSH-c
S_0
S_1
$S_2 \times 40$
probability
1.0
0.5
0.0
0
10
20
30
momentum (a.u.)
momentum (a.u.)

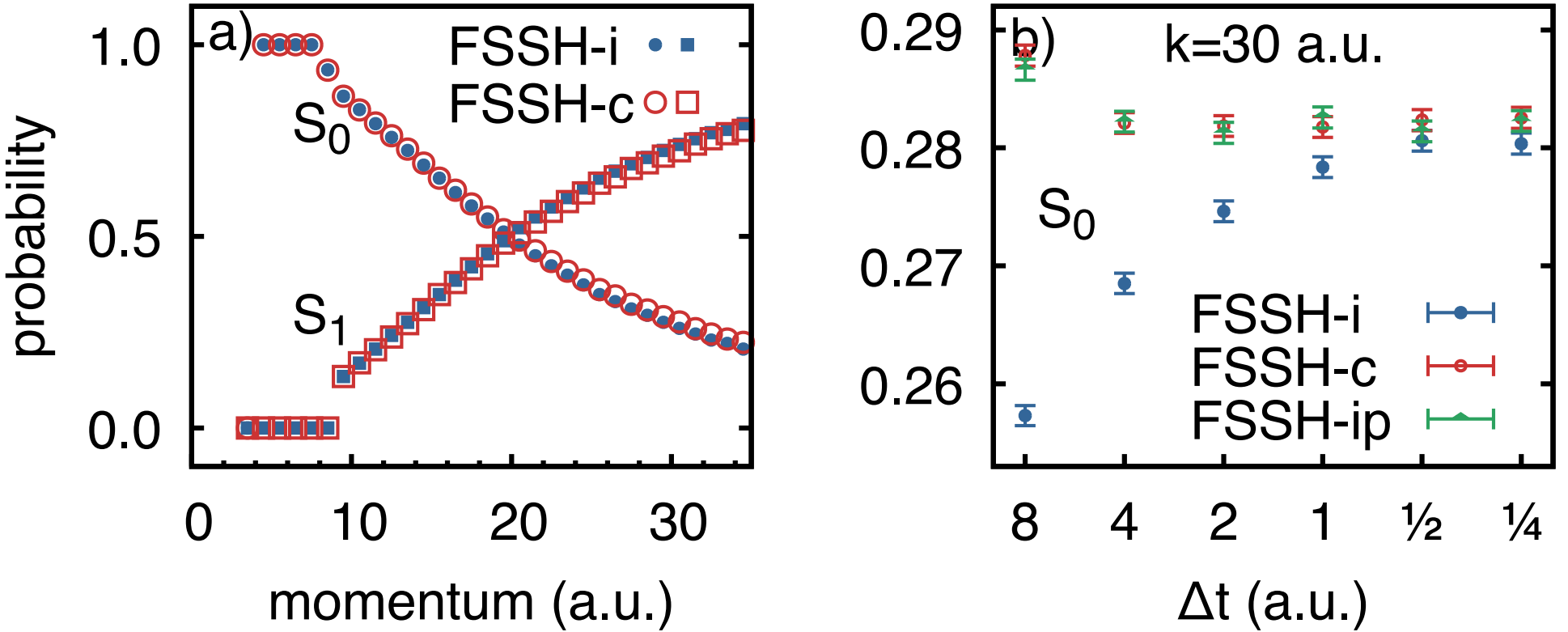
a)
FSSH-i
FSSH-c
S_0
S_1
probability
1.0
0.5
0.0
0
10
20
30
momentum (a.u.)
b)
k=30 a.u.
S_0
FSSH-i
FSSH-c
FSSH-ip
0.29
0.28
0.27
0.26
8
4
2
1
½
¼
Δt (a.u.)

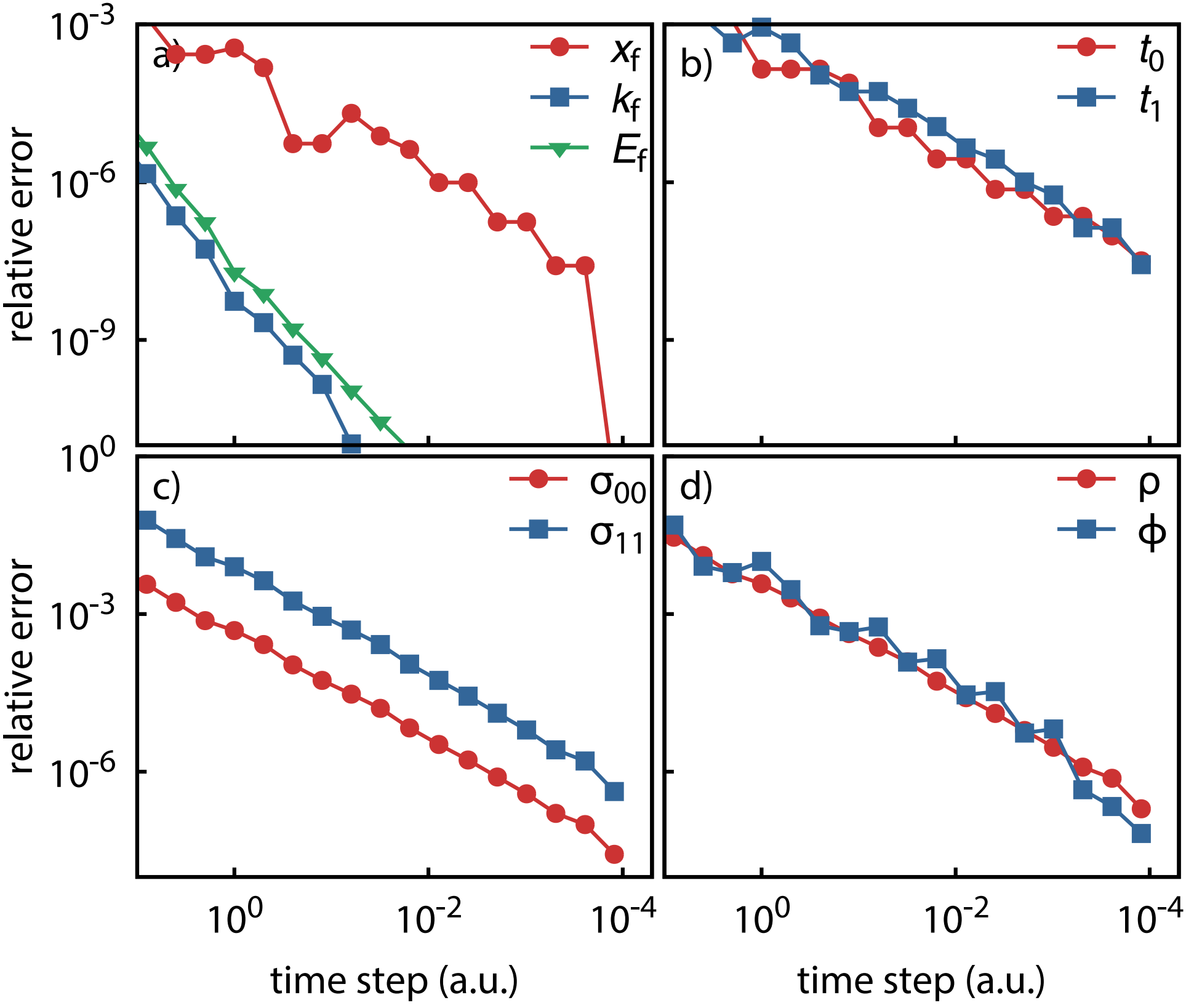
a)
b)
c)
d)
x_f
k_f
E_f
t_0
t_1
σ_{00}
σ_{11}
ρ
ϕ
relative error
relative error
10^{-3}
10^{-6}
10^{-9}
10^{0}
10^{-3}
10^{-6}
10^{0}
10^{-2}
10^{-4}
10^{0}
10^{-2}
10^{-4}
time step (a.u.)
time step (a.u.)

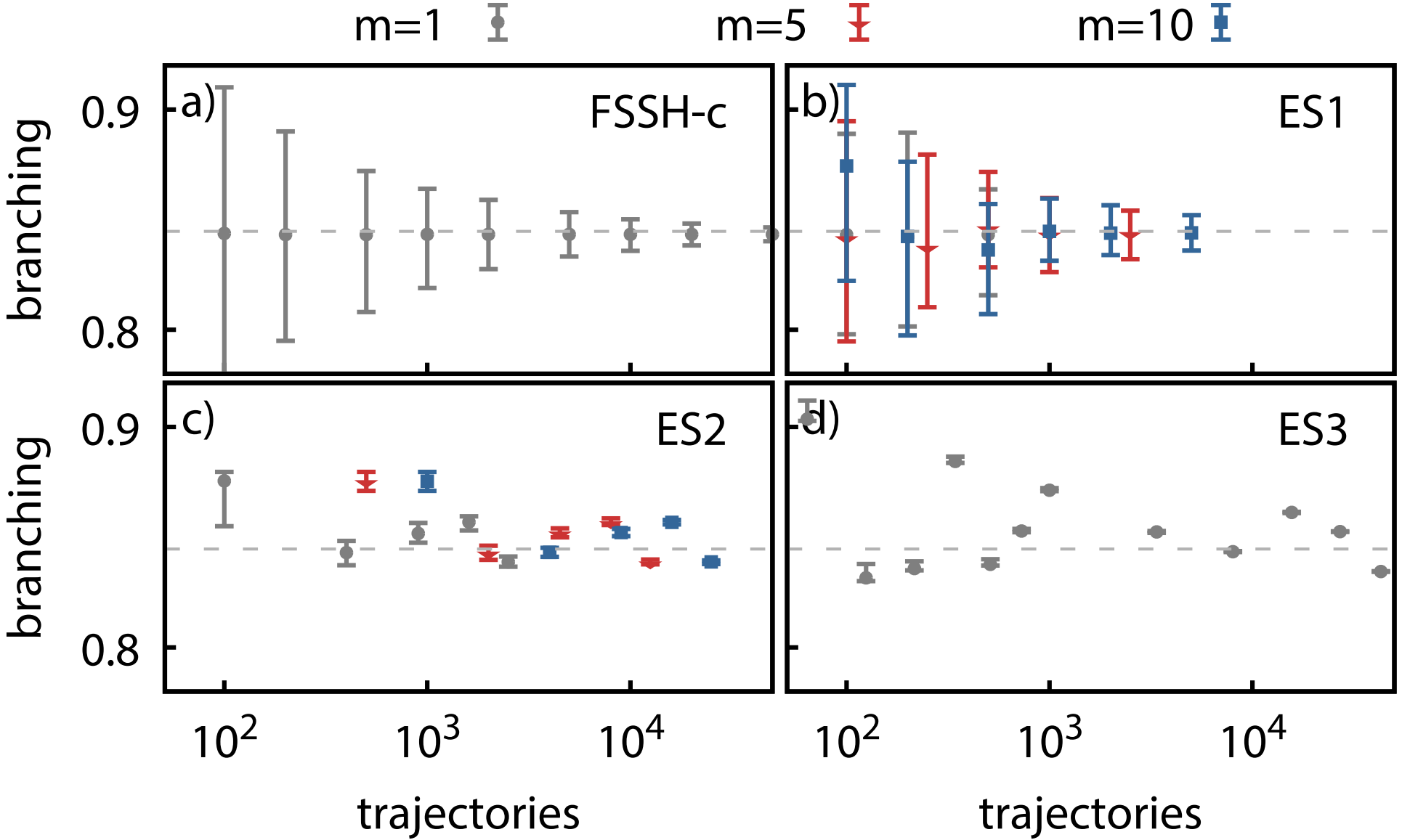
m=1
m=5
m=10
a)
FSSH-c
b)
ES1
c)
ES2
d)
ES3
branching
0.9
0.8
10^2
10^3
10^4
trajectories

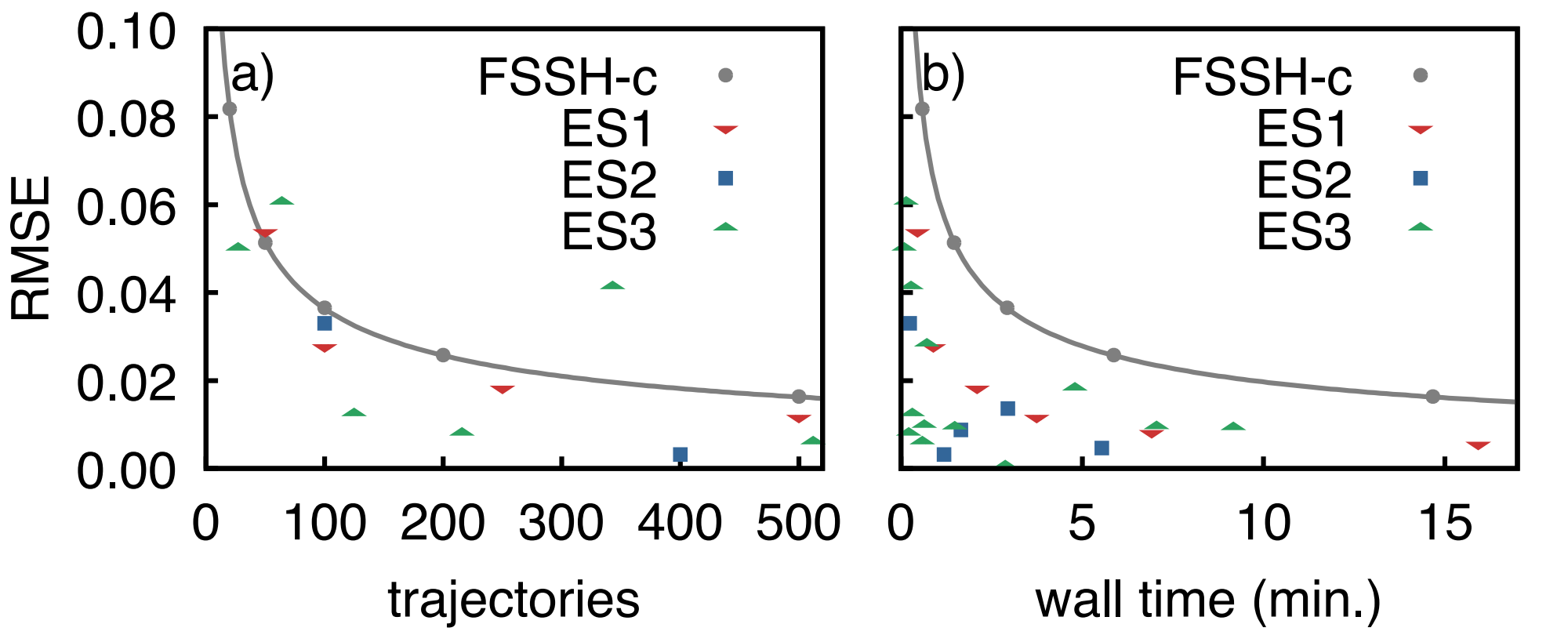
a)
b)
FSSH-c
ES1
ES2
ES3
RMSE
0.10
0.08
0.06
0.04
0.02
0.00
0
100
200
300
400
500
5
10
15
trajectories
wall time (min.)

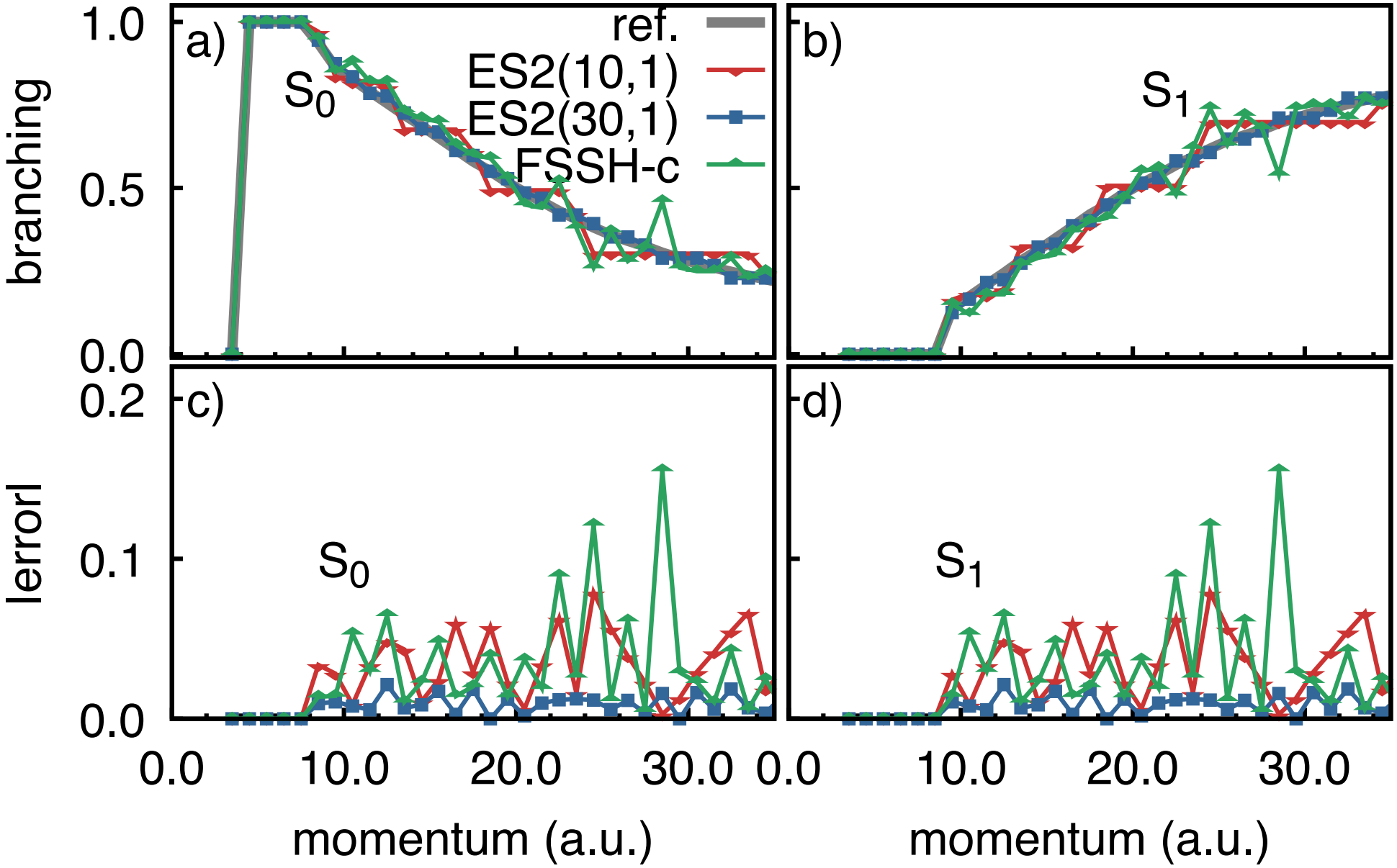
a)
b)
c)
d)
ref.
ES2(10,1)
ES2(30,1)
FSSH-c
S0
S1
S0
S1
branching
lerrorl
1.0
0.5
0.0
0.2
0.1
0.0
0.0
10.0
20.0
30.0
0.0
10.0
20.0
30.0
momentum (a.u.)
momentum (a.u.)